

# PORE-SCALE DISPLACEMENT DURING FAST IMAGING OF SPONTANEOUS IMBIBITION

W.-B. Bartels<sup>1,5</sup>, M. Rücker<sup>2,5</sup>, M. Boone<sup>3</sup>, T. Bultreys<sup>2,4</sup>, H. Mahani<sup>5</sup>, S. Berg<sup>5</sup>, S.M. Hassanizadeh<sup>1</sup> and V. Cnudde<sup>4</sup>

<sup>1</sup> Earth Sciences department, Utrecht University, 3584 CD Utrecht, NL

<sup>2</sup> Department of Earth Science and Engineering, Imperial College London, SW7 2AZ UK

<sup>3</sup> XRE, Technologiepark-Zwijnaarde, 9052 Ghent, BE

<sup>4</sup> UGCT- PProGRes, Ghent University, Krijgslaan 281 S8, 9000 Ghent, BE

<sup>5</sup> Shell Global Solutions International B.V., Kesslerpark 1, 2288 GS Rijswijk, NL

*This paper was prepared for presentation at the International Symposium of the Society of Core Analysts held in Vienna, Austria, 27 August – 1 September 2017*

## ABSTRACT

Amott spontaneous imbibition tests are well-established methods to investigate wettability and wettability alteration in oil saturated rock samples. Usually the cumulative volume of produced oil versus time is used as qualitative indicator of the wettability or wettability alteration of the sample. In this study, we used fast X-ray CT imaging aimed at linking the observed oil production to underlying pore-scale processes. In this study, we developed novel core holders suited for HECTOR (Higher Energy CT Optimized for Research) micro-CT scanner and EMCT (Environmental Micro-CT) scanner from the Centre for X-ray Tomography of the Ghent University (UGCT). We demonstrate these capabilities for a crude oil-brine-carbonate rock (Ketton) system to visualize the pore-scale fluid distribution during Amott tests. We performed experiments on mini-plugs (diameter: 4 mm, length: 20 mm) to capture dynamic processes during spontaneous imbibition by fast imaging (up to 15s per full rotation) with a voxel size of 13  $\mu\text{m}$  and SCAL plugs (diameter: 2.54 cm, length: 5 cm). We monitored oil configuration changes over a period of several months, to verify consistency of oil production behaviour across length scales. After initialization with oil and water, the samples were surrounded by formation water for imbibition. From 3D reconstructed and segmented images, we observed movement of the oil phase in the pore space of the rock in real time in water-wet (mini-plug and SCAL plug) and mixed-wet (SCAL plug) systems. Both the mini-plug and SCAL plug seemed to show preferred production sites. Furthermore, the pore-scale images of the mini-plug showed production due to snap-off in boundary adjacent pores. The pore-scale information aids in assessing the standard sample preparation and handling protocols in Amott tests. Moreover, the pore-scale information was used to interpret the cumulative production versus time curve of the SCAL plugs.

## INTRODUCTION

Spontaneous imbibition is the capillary-driven invasion of wetting-phase into the pre-

space of a porous medium, thereby displacing a non- or less-wetting phase initially in place. This process is seen in daily life when ink sinks into paper or water infiltrates soils. The process is also relevant in petroleum engineering. For instance, spontaneous imbibition occurs in an unsteady state displacement where in absence of capillarity we have a shock-front, but in presence of capillarity the shock-front becomes a smooth curve. Also, spontaneous imbibition plays a role in recovering oil from matrix blocks surrounded by fractures.

The imbibition capillary pressure-saturation curve consists of a forced and a spontaneous part. The forced part is measured in centrifuge or porous plate set-up. The spontaneous part is measured in tests such as the Amott test [1, 2], see Figure 1a, which ultimately provides a value for the saturation at a capillary pressure of zero. These laboratory tests are numerous [3-6]. The main variable that is measured in these tests is cumulative oil production versus time, see Figure 1b. With the part of the capillary pressure curve obtained from this data, these tests aim to indicate the (change of the) wettability state by assigning an index to the crude oil, brine, rock (COBR) system, see Figure 1c. Since wettability influences flow behavior, an accurate representation of the wettability of a rock type is imperative in predicting flow dynamics.

To make sure the variation in capillary pressure curves is because of wettability, different scaling groups were proposed to eliminate the effect of initial water saturation, mobility and viscosity, and interfacial tension variations, e.g. [7-9], on the cumulative production versus time curves. It has been shown that in many cases of uniform wettability, the scaling groups are effective [8]. However, [10] has shown that natural systems are most likely mixed-wet systems because of the connate water that is in the pore-space which prevents direct contact between oil and rock. Besides, there are general problems with wettability indices. For instance, indices computed from the Amott and USBM methods are often misleading when it comes to predicting sample wettability and associated flow behavior [11]. One reason for this is that the index represents a non-unique measure of wettability since different combinations may lead to the same index.

In summary, at least for mixed-wet systems, the wettability index that followed from curves of total production versus time, may not reflect the wettability following from the sum of the local pore-space wettability states. Since wettability finds its origin below the core scale, this is not necessarily surprising. Therefore, interpretation of the production curves and consequently wettability may be improved by adding the pore-scale information, as suggested by [12]. In addition, pore-scale information can be used to verify the experimental protocols for Amott tests. Issues like trapped gas or a significant capillary end-effect that may impact the result can be detected. In this study, we use SCAL plugs to examine those two effects.

Finally, there is the fundamental question about where and how the oil is produced from the sample. To address this question, we use a water-wet mini plug, because there is often no onset before spontaneous imbibition starts in water-wet systems. This eliminates some uncertainty in monitoring the dynamics of spontaneous imbibition. The visualized volume contains both (part of) the sample and the surrounding fluid, making this a suitable dataset for pore-scale simulation of the imbibition process as suggested by [12].

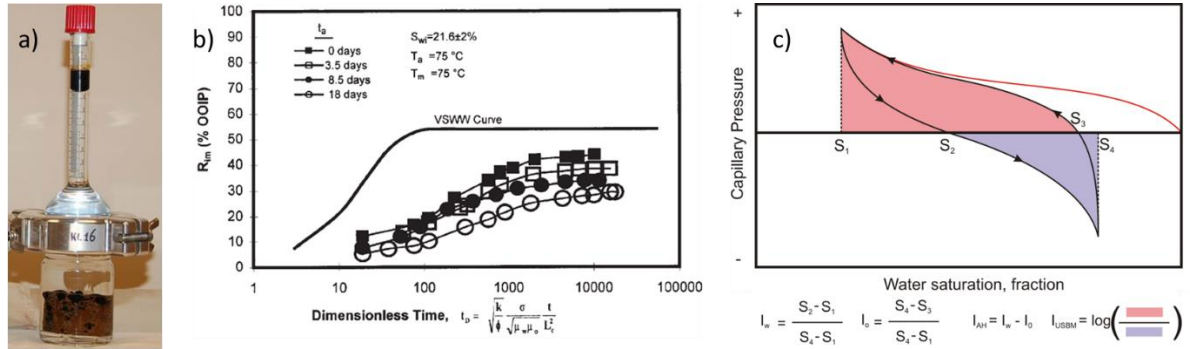


Figure 1: a) Amott spontaneous imbibition test with all faces open. b) Example of spontaneous imbibition oil production versus time and as function of ageing, after [3]. c) Definitions of wettability indices, taken from [13].

We used three novel set-ups in combination with HECTOR and EMCT micro-CT scanners [14, 15]. The imaging systems were developed by the Centre for X-ray Tomography of the Ghent University (UGCT, [www.ugct.ugent.be](http://www.ugct.ugent.be)) in collaboration with XRE ([www.xre.be](http://www.xre.be)). They were used to visualize the pore-scale fluid distribution during Amott tests. We present pore-scale behavior as well as the observed cumulative oil production versus time curves.

## MATERIALS AND METHODS

### Crude oil, brine, rock systems

For the experiments, we used Ketton carbonate (Oolite) rock [16], porosity  $\Phi_{MICP} = 23\%$  and  $K_{brine} = 5.7$  Darcy, formation water (FW) (density  $\rho = 1.152$  g/cm<sup>3</sup>, viscosity  $\mu = 1.550$  mPa·s, at  $T = 20^\circ\text{C}$ , composition see Table 1), decane ( $\rho = 0.730$  g/cm<sup>3</sup>,  $\mu = 0.920$  mPa·s, at  $T = 20^\circ\text{C}$ ) and crude oil ( $\rho = 0.8833$  g/cm<sup>3</sup>,  $\mu = 11.486$  mPa·s, at  $T = 20^\circ\text{C}$ , composition see Table 2). Both decane and crude A were doped with 20 wt% Iodo-decane to obtain higher X-ray attenuation.

Table 1: Composition of FW

Ion	Na <sup>+</sup>	K <sup>+</sup>	Mg <sup>2+</sup>	Ca <sup>2+</sup>	Sr <sup>2+</sup>	Cl <sup>-</sup>	SO <sub>4</sub> <sup>2-</sup>	HCO <sub>3</sub> <sup>-</sup>	TDS	Ionic Strength [mol/L]	pH
FW [mg/L]	49.9	0	3.25	14.5	0	112	234	162	180	3.659	6.9

Table 2: Crude oil specification

IFT FW – doped crude oil	TAN (mg KOH/g)	TBN (mg KOH/g)	Asphaltene (g/100ml)
20 mN/m @ 20°C	0.5	1.0	0.244

A list of systems used in this study, together with their initialization methods can be found in Table 3. The mini-plugs were difficult to machine to the desired diameter; they would easily break. Therefore, the mini-plugs that survived contained a higher volume percentage of cement compared to the SCAL plugs. Cement contains micro-porosity that

cannot be resolved in the used micro-CT scanners and can make up to 40% of the total porosity in Ketton (see Figure 3) which is consistent with the initial water saturations for the SCAL plugs. In that case, the role of the water saturated micro-porosity is limited to slightly increasing the water connectivity. In addition, since the pores in the observable pore-space are well connected, there should not be events in the micro-pores.

*Table 3: List of samples used in this paper. We used two types of plugs: small SCAL plugs (5 cm length and 2.54 cm diameter) and mini-plugs (20 mm length and 4 mm diameter). The initial water saturation ( $S_{wi}$ ) excludes the water in the micro-pores for the mini-plug. The oil phases were doped with 20 wt% Iodo-decane.*

Rock	Oil phase	$S_{wi}$	Desaturation	Ageing	Wetting
KET1_06	Decane	0.37	Centrifuge	40°C/24 hrs	Water-wet
KET1_08	Crude oil	0.34	Centrifuge	40°C/24 hrs	Mixed-wet
KET1_09	Crude oil	0.38	Centrifuge	40°C/24 hrs	Mixed-wet
Mini-plug	Crude oil	0.06	Flooding	40°C/24 hrs	Water-wet

### *Experimental workflow*

#### *Sample saturation*

Both the SCAL plugs and the mini-plugs were saturated by placing the samples in a sleeve and applying vacuum ( $\sim 10^{-2}$  mbar). Subsequently, de-aerated FW was added. As final step, the samples were placed in a pressure chamber at 30 bars for two hours to dissolve any gas bubbles that may still exist in the sample.

#### *Sample desaturation: centrifuge and micro-coreholder*

The SCAL plugs were brought to initial water saturation in a centrifuge (URC-628, Coretest Systems Inc., used at 3500 RPM for SCAL plugs) in 24 hours. To prevent gradual heating during centrifuging, the temperature was fixed at 40°C. By automatic recording of the production and material balance calculation, initial water saturations shown in Table 3 were achieved. Because centrifuging was done at elevated temperature, aging of the rock took place for the samples saturated with crude oil. Therefore, we ended up with one water-wet SCAL plug and two mixed-wet SCAL plugs, see Table 3.

For the mini-plug, we used a specially designed micro-coreholder to (de-)saturate the samples by flooding, see Figure 2a. The core holder consisted of Hastelloy steel and X-ray transparent polyether ether ketone (PEEK). This way, the saturation state of the sample could be monitored during or after (de-)saturation. The bottom of the cell consisted of a pressure vessel that regulated the sleeve pressure, which was set by water (up to 30 bars). Because of the pressure vessel there was no need to keep any pressure line attached to the set-up, allowing 360 degrees rotation in a micro-CT scanner. The micro-coreholder could be used for both static (e.g. aging tests) and dynamic (e.g. flow tests) experiments at elevated temperatures up to 80°C. Properties of the mini-plug can be found in Table 3.

#### *Experimental protocols*

We used standard experimental protocols for SCAL spontaneous imbibition tests. An exception was the aging for SCAL plugs as addressed above. One part of the SCAL plug Amott protocol is to roll the sample on a tissue saturated with oil to remove oil attached to the outside of the sample. However, this may create suction on the surface pores if the

tissue is not wet enough or it may not remove all oil from the outside of the sample when the tissue is too wet. Both scenarios may influence the cumulative oil production versus time curve. Still, it was decided to adhere to the standard protocols. For mini-plugs, similar protocols were used. However, because of the small volume of resolvable pore space and because the production was not measured, it was decided to refrain from rolling this sample. In addition, because spontaneous imbibition may be a sub-second process, it is relevant to note that the delay between filling the cells with brines and starting of the scans was around one minute for the mini-plugs and around five minutes for the SCAL plugs.

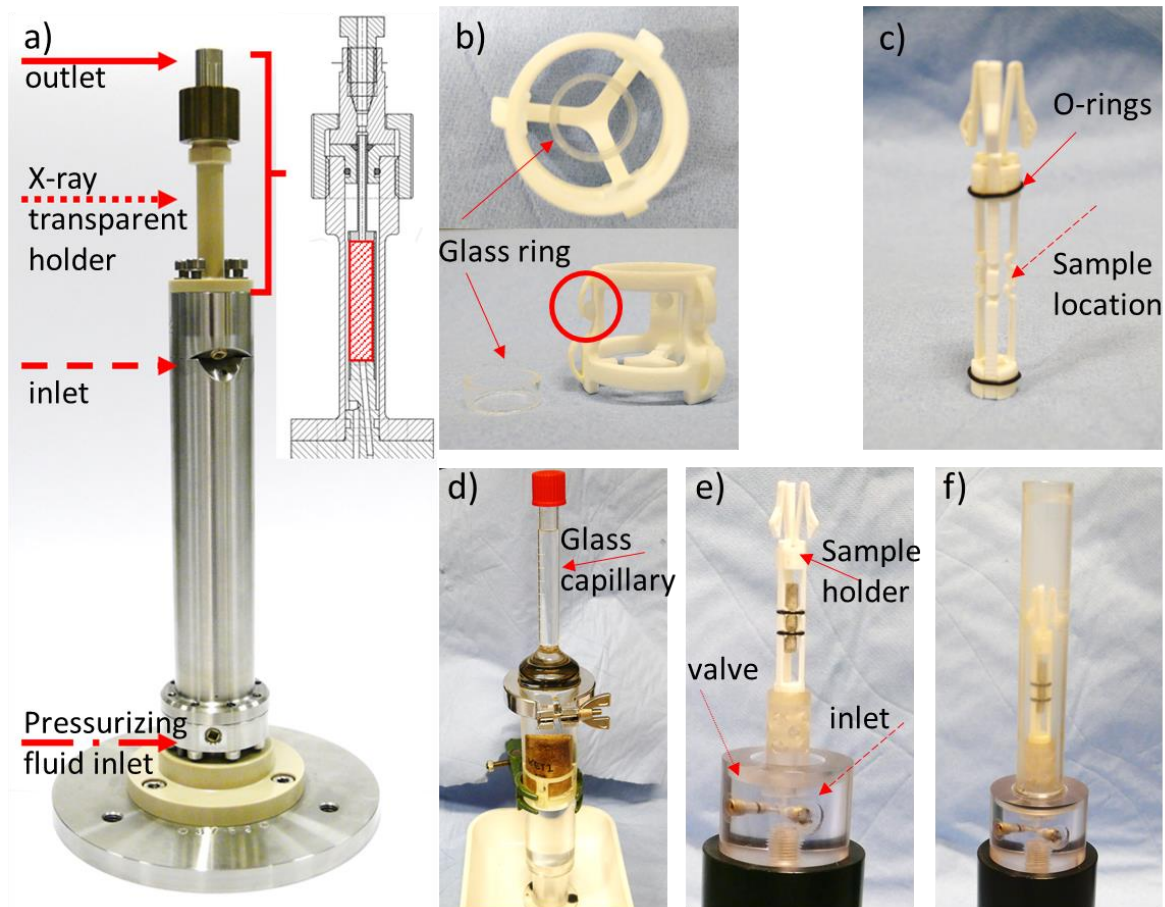


Figure 2: a) Micro-coreholder for de-saturation of mini-plugs and flow experiments. The bottom cylinder is a pressure vessel, with water as pressurizing agent. The PEEK top holds the sample and allows for X-ray scanning. This section is shown again in the inset in which a typical mini-plug ( $4 \text{ mm} \times 20 \text{ mm}$ ) is indicated by the red square. Flow lines for de-saturation can be attached at the top and bottom of the PEEK section. Sample holders for the spontaneous imbibition cells (b, c) and the Spontaneous imbibition cells for SCAL (d) and mini-plug (e, f).

### Spontaneous imbibition set-ups

Two different set-ups were used for spontaneous imbibition: one for the SCAL plug Amott tests (a slightly modified standard Amott cell) and one for the mini-plug Amott test, see Figure 2d-f. Both cells can be used for different types of spontaneous imbibition tests and are made of crude-oil-resistant and X-ray-transparent materials. For all faces

open spontaneous imbibition tests, the rock sample needs to be well consolidated. For other types of imbibition experiments (one end open or two ends open) a sleeve can be used, which also poses less stringent requirements on the consolidation state of the sample. The cells can handle samples of various sizes.

The sample holders – depicted in Figure 2b, c – that are placed in the cell are constructed to minimize contact with the sample whilst simultaneously fixing the sample position in the cell. It is vital that the samples do not move during the scans to prevent blurring of the images. In the case of the SCAL plugs, the points where the sample holder touches the sample were made of water-wet glass to prevent oil from spreading along the holders.

#### *Micro-CT scanners: HECTOR and EMCT*

HECTOR [14], was used for time lapse imaging of the SCAL plugs. The X-ray tube was operated at 160 kV with a power of 14 W. The plug was imaged using 4 consecutive scans along the vertical axis of the sample, which were merged together, resulting in a total reconstructed volume of  $2000 \times 2000 \times 4700$  voxels, with a voxel size of  $14.25 \mu\text{m}$ . Individual consecutive scans were used to reduce the scan time (100 minutes per scan) and limit motion blurring during the acquisition.

EMCT, also known as the Environmental MicroCT scanner [15], was used for fast dynamic imaging of the mini-plugs. Unlike conventional micro-CT systems, the sample remains immobile in the EMCT, while the X-ray tube and detector rotate around the samples in a horizontal plane. This fixed sample configuration makes the system ideal for continuously monitoring dynamic in-situ processes. The mini-plugs were imaged at different spatial and temporal resolutions related to the assumed rate of the process that was monitored. The onset of the imbibition was imaged with a high temporal resolution of 15 seconds for a full rotation and a spatial resolution of  $13 \mu\text{m}$ . Later stages of the process were imaged at a spatial resolution of  $6.7 \mu\text{m}$  and a temporal resolution down to 70 seconds for a full rotation.

#### *Image analysis*

All scans were reconstructed using the dedicated reconstruction tools in the Aquila software package from XRE. Further post-processing and visualization of the data were done using Avizo 9.2.0 (FEI) and GeoDict, (Math2Market). The images were first filtered with a non-local means filter and subsequently segmented by comparing the data of the dry scan with the wet scans captured during the spontaneous imbibition experiment, following the procedure described in [17].

## **RESULTS AND DISCUSSION**

### *Verification of the production curve in SCAL-sized samples and Amott protocols*

In the initial state of both the SCAL and the mini-plugs, no air was observed throughout the sample, indicating that the standard procedures to initialize plugs were correct and working. For all samples, no capillary-end effect was detected even though the centrifuge was used for the SCAL plugs. This is based on estimations made using the mercury intrusion porosimetry curve and the centrifuge inlet pressure, see Figure 3. However, we observed a considerable amount of cement in the matrix in the micro-CT images, giving rise to a large fraction of micro-porosity which may influence the results. The cement is difficult to indicate in wet samples, because the attenuation is close to that of the oil

phase. Rolling the samples on a tissue pre-wetted with oil, did not seem to have any effect on the interior of the sample.

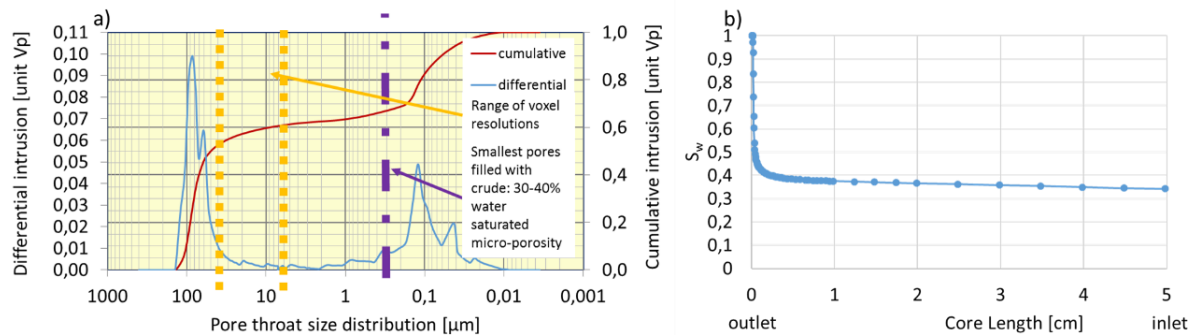


Figure 3: a) Mercury intrusion curve of one of the SCAL Ketton samples. The dotted lines indicate the voxel resolutions of the different scans that were made. The dash-dot line indicates the smallest pores filled with crude by the centrifuge. All scans capture the larger pores and are well above the sizes of the micro-porosity. In b) the estimation of the capillary end effect along the length of the SCAL plug.

For the mini-plugs, the sample holder (Figure 2c and Figure 7) was oil-wet which means it may have led to draining of oil from near-surface pores. Therefore, only spontaneous imbibition that was isolated from other parts of the pore-space, i.e. disconnected oil that is moving out, could be examined.

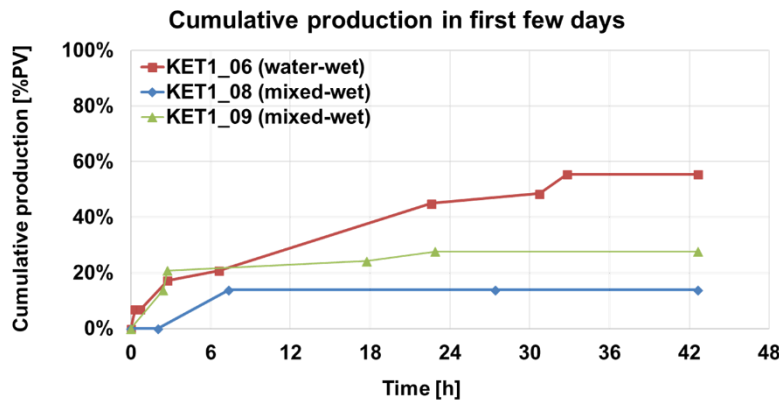


Figure 4: All production in % of visible pore volume, for both water-wet and mixed-wet samples, occurs right after immersion in brine. KET1\_08 was kept for a total of 122 days in which no additional production occurred. The wettability state of the samples is based on the curves in this figure and on the pore scale images of protruding droplets (and their contact angle with rock surface) in Figure 5, Figure 8 and Figure 9.

Next, it was investigated whether the produced oil, as measured in the production curve, see Figure 4, reflected the pore-space of the sample as mentioned in [12]. The water-wet SCAL plug shows more production than the two mixed-wet SCAL plugs, see Figure 4. For the water-wet SCAL plug production coincides with pore-scale displacement as can be seen from the imbibition front in Figure 5b, c. For the mixed-wet case, production does not coincide with pore-scale changes in fluid configuration, as can be seen in Figure 5e, f and Figure 6. This means that the oil volume in the glass capillary reflects neither the rate at which the oil is produced nor the volume of produced oil, but probably relates to oil attached to the outside of the sample. To get a production of 1 ml, the film of oil covering the sides of the cylindrical plug would have to be ~0.25 mm thick. For the

water-wet plug we used doped decane. Therefore, the oil film on the sample is expected to be negligible. The production of the water-wet mini-plug was not measured but the significant amount of cement in the pore-space may explain the lack of response to brine exposure.

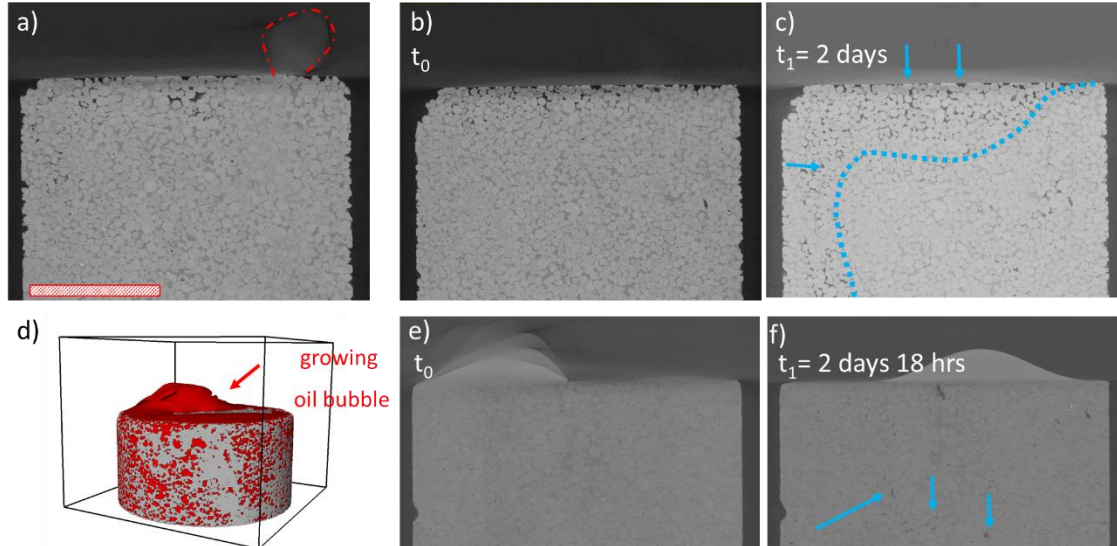


Figure 5: a, b, c) the water-wet SCAL sample (KET1\_06). The red bar in a) indicates 1 cm. d, e, f) a mixed-wet SCAL sample (KET1\_09). In a) and d-f) an oil droplet is seen growing at the top of the SCAL samples. b) initial saturation of water-wet SCAL sample at  $t_0 \sim 105$  minutes c) saturations after 2 days for the water-wet SCAL sample. A clear imbibition front has formed, indicated by the blue line and arrows. The center of the sample shows very little change. e) initial saturation of mixed-wet SCAL sample at  $t_0 \sim 105$  minutes. f) Almost no change in the mixed-wet sample after  $\sim 2$  days. The little change there is, is indicated by blue arrows.

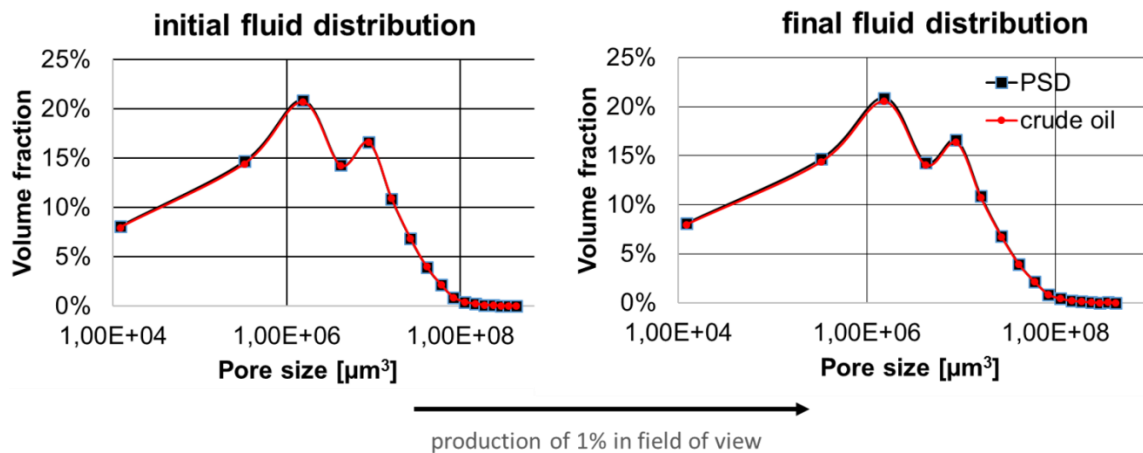


Figure 6: Change in oil distribution (red dotted line) compared to the Pore Size Distribution (PSD, black line with squares) for the mixed-wet SCAL plug (KET1\_09) in Figure 5e, f. The change is minimal whereas the production in the glass capillary at the top reaches almost 1 ml.

#### Observations from micro-CT images

The SCAL plugs, both water-wet and mixed-wet, showed large oil blobs protruding from the top, see Figure 5a, d–f, at a single location. Visual observation also indicated that the drop detached and grew back again several times for the water-wet case, which was in

line with the preferred production sites mentioned in [12]. The mixed-wet sample – in contrast to the water-wet sample – did not show an imbibition front. In addition, there was no significant change in the occupancy of the pores, whereas production was observed, see Figure 4 and Figure 6.

A similar observation was made for the mini-plug in Figure 7. However, because of the limited field of view (FOV) this cannot be confirmed. In the mini-plug, preferential production sites were also observed. The observed process has some similarity to that hypothesized by [12] when discussing the generation of capillary back pressure at a wetted open surface during imbibition. They stated that [18, 19] found that when air is the non-wetting phase it tends to “...emerge as a stream of very fine bubbles, often at a single location, which indicates that snap-off is occurring a short distance in from the open face.” The stream of fine and larger bubbles was observed by eye, but it was not possible to image this, because it fell out of the FOV for the mini-plug or out of the temporal resolution for the SCAL plug. However, the bubble that emerged in our FOV of the mini-plug shows snap-off at a short distance from the open face, see Figure 8.

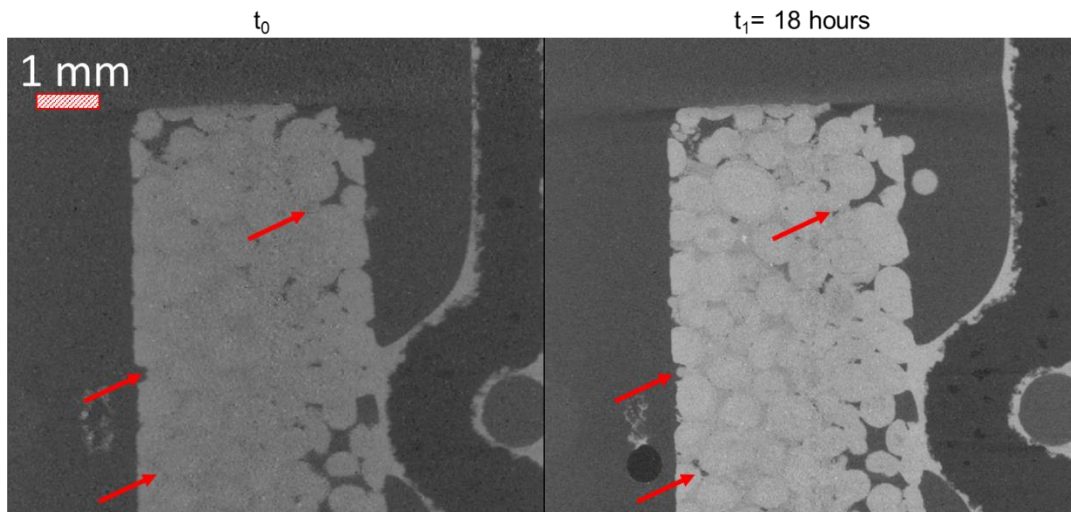


Figure 7: Spontaneous imbibition dynamics in the water-wet mini-plug are indicated by the red arrows. The sample holder is also clearly visible. The bright phase coating the holder is doped crude oil.

#### *The effect of buoyancy on spontaneous imbibition*

We observe that the outside of the mixed-wet SCAL sample is covered with crude oil, see Figure 9a. However, there seems to be less crude towards the bottom of the sample. Combined with the imbibition front observed in Figure 5c and the rising oil drop observed in the mini-plug, see Figure 8, this could mean that gravity effects dominate the imbibition process in our samples. However, the buoyancy/capillary force computation in Figure 9b indicates otherwise: it shows that for oil clusters of a length equal to that of the sample, gravity forces are an order of 10,000 less than capillary forces. Buoyancy would dominate inside the pore space for contact angles around 90 degrees. However, the effect of contact angle in the force balance is uncertain, since advancing and receding contact angles may show significant hysteresis, see e.g. [20]. When oil starts protruding from the sample, the restrictions of the pore-space fall away and gravity dominates over capillary

forces. Buoyancy may play a role in ‘sucking out’ oil and creating space for water to imbibe as indicated in Figure 8. Depending on the crude oil and liquid-liquid interface properties (such as interface elasticity, interfacial tension, composition), and pore geometry, the protruding oil drop may grow before snap-off disconnects the drop from the interior of the sample, see Figure 8b, c. Interestingly, after snap-off, the droplet retains a non-equilibrium shape for minutes (Figure 8c), before moving toward a more stable configuration on the rock surface (Figure 8d).

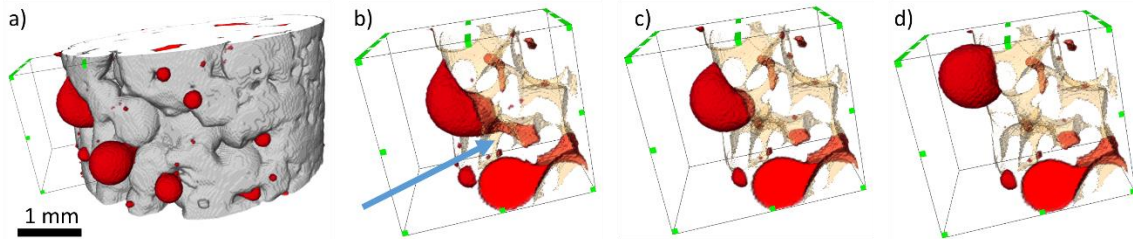


Figure 8: Oil droplet movement out of pore space and snap-off event in mini-plug. a) shows the grains (white) and oil (red) configuration in the plug. b-d shows time steps of 11 minutes, 4 hours after starting the experiment. The snap-off event is clearly visible between steps b) and c) [indicated by the blue arrow]. From c) to d) the drop moves towards a more spherical/equilibrium shape.

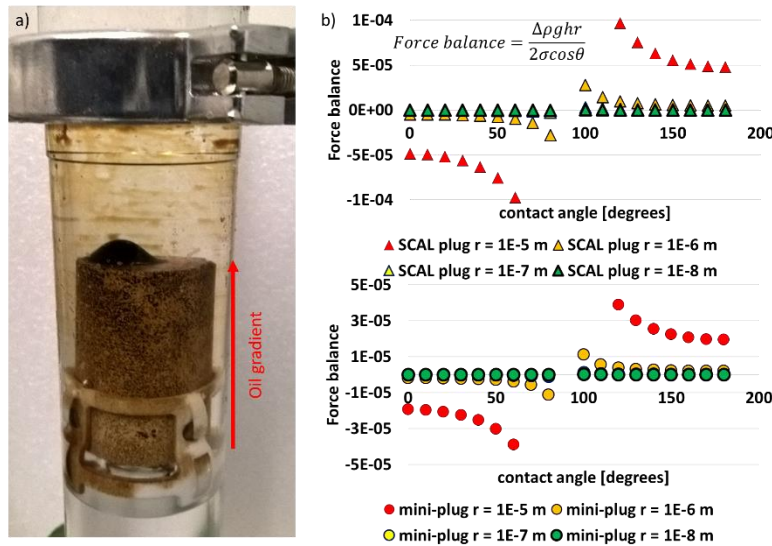


Figure 9: a) SCAL plug (KET1\_09) showing gradient of oil coverage on the outside of the sample which cannot be due to centrifuge desaturation. Notice also the bubble on top. Together with the dynamics of production in the mini-plug, see Figure 8 this hints that buoyancy is important in spontaneous imbibition of this rock b) Computation shows that gravity drainage is very unlikely inside both samples for  $h$ =sample/cluster length,  $\Delta\rho$ = density difference of fluid phases,  $\sigma$ =interfacial tension,  $\theta$  = contact angle, and  $r$ =pore diameter.

## CONCLUSION

We used three novel coreholders and fast benchtop micro-CT scanners to study spontaneous imbibition both on long (months) and short time scales (seconds to minutes). From 3D reconstructed and segmented images, we observed movement of the oil phase in the pore space of the rock in water-wet (mini-plug and SCAL plug) and mixed-wet (SCAL plug) systems using benchtop X-ray micro-tomography.

We found the *sample preparation* protocols to be adequate i.e. no air bubbles were trapped in the pore space and homogeneous oil saturations were achieved. However, we showed that there is a discrepancy between production as measured in the capillary of the Amott cell and the pore-scale observations in some SCAL plugs. The fluid distribution in the interior of the plugs remained unchanged whereas production was still accumulating in the capillary. The produced oil may have come from the oil layer attached to the outside of the sample: a rough estimate indicates an oil film of ~0.25 mm would be sufficient to produce 1 ml of oil. In that sense, rolling the sample per protocol may still influence the production curves even though the rolling did not seem to affect the pore space distribution of oil. For water-wet plugs, the measured production matches the observed pore-scale events better. Since we used decane in this case, the oil film on the sample is expected to be negligible because of the water-wetness of the system. For both cases, oil drops would protrude from the sample without being recovered.

Furthermore, we observed an ‘oil gradient’ on the outside of the sample (mixed-wet SCAL plug), a big oil droplet on the top of both water-wet and mixed-wet SCAL plugs and a pore-scale snap-off event in the water-wet mini-plug. In addition, we observed preferred production sites for all water-wet samples. They all hint that buoyancy is important for the displacement of oil. However, force balance computations show that buoyancy is not important inside the samples, but may be very important outside of the sample as demonstrated by the mini-plug pore-scale imbibition.

The next part of this study focusses on investigating spontaneous imbibition when changing brine salinity. This finds its application in Amott tests that are conducted to investigate the response of a COBR system to Low Salinity Flooding.

## ACKNOWLEDGEMENTS

We would like to acknowledge the staff of UGCT, Ghent, Belgium for support during the execution of this work. We thank Alex Schwing and Rob Neiteler for the creation of the flow set-up and instrumentation, Fons Marcelis and Ab Coorn for sample preparation, and Kamaljit Singh from Imperial College London for supplying the Ketton rock.

## REFERENCES

1. Amott, E., “Observations relating to the wettability of porous rock”, *Petroleum Transactions*, AIME (1959).
2. Donaldson, E.C., R.D. Thomas and P.B. Lorenz, “Wettability Determination and Its Effect on Recovery Efficiency”, *SPE Journal* (1969), March, 13-20.
3. Tang, C.Q., and N.R. Morrow, “Salinity, Temperature, Oil Composition and Oil Recovery by Waterflooding”, This paper was presented at the SPE Annual Technical Conference and Exhibition held in Denver, Colorado, 6-9 October 1997.
4. Zhou, X., N.R. Morrow and S. Ma, “Interrelationship of Wettability, Initial Water Saturation, Aging Time and Oil Recovery by Spontaneous Imbibition and Waterflooding”, *SPE Journal* (2000), 5 (2), 199-207.
5. Graue, A., E. Aspenes, T. Bognø, R.W. Moe and J. Ramsdal, “Alteration of wettability and wettability heterogeneity”, *Journal of Petroleum Science and Engineering* (1999), **33**, 3-17.

6. Fischer, H., and N.R. Morrow, "Spontaneous Imbibition with Matched Liquid Viscosities", This paper was presented at the SPE Annual Technical Conference and Exhibition held in Dallas, Texas, U.S.A., 9-12 October 2005, *SPE* 96812.
7. Mattax, C.C. and J.R. Kyte, "Imbibition oil recovery from fractured water-drive reservoir", *SPE Journal* (1962), June, 177-184.
8. Ma, S., N.R. Morrow, and X. Zhang, "Generalized scaling of spontaneous imbibition data for strongly water-wet systems", *Journal of Petroleum Science and Engineering* (1997), **18**, 165-178.
9. Schmid, K.S., and S. Geiger, "Universal scaling of spontaneous imbibition for arbitrary petrophysical properties: Water-wet and mixed-wet states and Handy's conjecture", *Journal of Petroleum Science and Engineering* (2013), **101**, 44-61.
10. Salathiel, R.A., "Oil Recovery by Surface Film Drainage In Mixed-Wettability Rocks", *Journal of Petroleum Technology* (1973), 1216-1224.
11. Dixit, A.B., J.S. Buckley, S.R. McDougall and K.S. Sorbie, "Core wettability: should  $I_{AH}$  Equal  $I_{USBM}$ ", *SCA9809* (1999).
12. Mason, G., and N.R. Morrow, "Developments in Spontaneous Imbibition and possibilities for future work", *Journal of Petroleum Science and Engineering* (2013), **110**, 268-293.
13. Abdallah, W., J.S. Buckley, A. Carnegie, J.E.B. Herold, E. Fordham, A. Graue, T. Habshy, N. Seleznev, C. Signer, H.Hussain, B. Montaron, and M. Ziauddin, "Fundamentals of wettability", *Oilfield Review* (2007), **19** (2), 44 - 61.
14. Dierick, M., D. van Loo, B. Masschaele, J. Van den Bulcke, J. Van Acker, V. Cnudde and L. Van Hoorebeke, "Recent micro-CT scanner developments at UGCT", *Nuclear Instruments and Methods in Physics Research B* (2014), **324**, 35-40.
15. Bultreys, T., W. de Boever, and V. Cnudde, "Imaging and image-based fluid transport modeling at the pore scale in geological materials: A practical introduction to the current state-of-the-art", *Earth-Science Reviews* (2016), **155**, 93-128.
16. Muir-Wood, H.M., 1952, "Some Jurassic Brachiopoda from the Lincolnshire limestone and upper estuarine series of Rutland and Lincolnshire", *Proceedings of the Geologists' Association* (1952), **63** (2), 113-42.
17. Berg, S., R.T. Armstrong, H. Ott, A. Georgiadis, S.A. Klapp, A. Schwing., R. Neiteler, N. Brussee, A. Makurat, L. Leu, F. Enzmann, J.-O. Schwarz, M. Wolf, F. Khan, M. Kersten, S. Irvine and M. Stampanoni, "Multiphase flow in porous rock imaged under dynamic flow conditions with fast X-ray computed microtomography". *Petrophysics* (2014), **55** (04), 304-312.
18. Unsal, E., G. Mason, N.R. Morrow, D.W. Ruth, "Bubble snap-off and capillary-back pressure during counter-current spontaneous imbibition into model pores", *Langmuir* (2009), **25** (6), 3387-3395.
19. Li, Y., G. Mason, N.R. Morrow, D.W. Ruth, "Capillary Pressure at the Imbibition Front During Water-Oil Counter-Current Spontaneous Imbibition", *Transport in Porous Media*, **77**, 475-487.
20. Raeesi, B., N.R. Morrow and G. Mason, "Effect of surface roughness on wettability and displacement curvature in tubes of uniform cross-section", *Colloids and Surfaces A: Physicochemical and Engineering Aspects* (2013), **436**, 392 - 401.